Automotive Science and Engineering, Volume 12, Issue 1, P 3737-3749

Iran University of Science and Technology

Automotive Science and Engineering

Journal Homepage: ase.iust.ac.ir

ISSN: 2717-2023

An experimental investigation on the effects of severely plastic deformation process on the mechanical properties of automotive resistance spot welded aluminum joints

Hamed Saeidi Googarchin*, Pouyan Namdar, Seyed Hooman GhasemiPourMasoule

Automotive Fluids and Structures Analysis Research Laboratory, School of Automotive Engineering, Iran University of Science and Technology, Tehran, Iran

ARTICLE INFO

Article history:

Received:

Accepted:

Published:

Keywords:

Constrained groove pressing

Automotive structure

Mechanical property

Pure aluminum

Resistance spot weld

A B S T R A C T

In this paper, the mechanical properties of welded single lap joints of pure aluminum sheets produced by severe plastic deformation (SPD) are considered. SPD in form of a large pre-strain was imposed on aluminum sheets through the constrained groove pressing (CGP) process. Furthermore, CGPed specimens are joined using the resistance spot welding (RSW) method. Welding time and force are maintained evenly. Welding current is raised until ideal failure mode is observed. Finally, mechanical properties of the fusion zone, heat affected zone (HAZ), and base metal of welded SPDed specimens are derived. The results show that by increasing the pre-strain in specimens, an improvement in yield strength, ultimate tensile strength, load carrying capacity, maximum displacement before failure, and nugget diameter is observed. Furthermore, the sensitivity of these parameters to the CGP pass number is considered. Finally, it has been shown that fusion zone and HAZ hardness values can increase by increasing the CGP pass number.

1. Introduction

Severe Plastic Deformation (SPD) proved to be an effective approach for increasing the strength of materials and strength in bulk shape without imposing defective pores and impurities [1]. Several SPD methods have been introduced to increase the strength of materials in bulks and sheets [2]. The constrained groove pressing (CGP) method presented by Shin et al. [3] has been used to impose plastic deformation in sheet metals. This process includes repetitive corrugating and flattening steps by certain grooved and flat dies. One pass of the CGP process includes four steps. First, the sheet undergoes a deformation by grooved die, then it is flattened using a flattening die. In the next step, the specimen is rotated 180° around its perpendicular axis and subjected to pressing of corrugated and finally flatten die again. Higher strain values can be achieved by introducing more CGP passes on the specimen. Many studies have been conducted around the evaluation of the CGP method on the improvement of sheet metal properties.

Saeidi Googarchin et al. [4] developed a hybrid method for analyzing CGP processed sheets. In addition, the effects of die parameters including

*Corresponding Author
Email Address:
hsaeidi@iust.ac.ir (H. Saeidi Googarchin)
https://doi.org/10.22068/ase.2021.589

groove angle, height, and width were investigated on processed sheets' mechanical properties. Kazeminezhad and Hosseini [5] developed a new FE code to investigate and propose an optimum die design in order to improve sheet mechanical properties. Results showed that the CGP process yields the highest strain magnitude in comparison to other GP process family. It was also found that in the first pass, CGP results in the least strain uniformity, but in subsequent passes, it leads to most strain uniformity.

In comparison to steel and other metals, lower density and weight coupled with its corrosion resistance gave rise to extensive usage of aluminum and its alloys in fabrication industries. The metal sheets have a vast application in the manufacturing of components and frames in the automotive and aerospace industries, where increasing the strength to weight ratio is important.

Shirdel et al. [6] studied a semi-CGP method imposed on pure aluminum sheets and presented the effects of different CGP passes on mechanical properties of specimens accompanied by FEM solutions. It was shown that the CGP process improves the mechanical properties of investigated sheets. Sajadi et al. [7] applied the CGP process to pure aluminum sheets to derive sheets' mechanical properties subjected to different sheet casings and die groove angles. Results show that increasing CGP passes improves the mechanical properties of the specimens.

One of the most important processes in the manufacturing of industrial components, automotive industries, in particular, is the joining of sheet metal parts. Many studies have been carried out to investigate the joining of SPDed materials.

Previous studies introduced friction stir welding (FSW) as one of the best methods to join SPDed materials, but the FSW method has proven to be difficult to apply not to mention in some industrial applications not possible for joining of components due to the high strength of CGP processed aluminum. Chen et al. [8] delved into the occurrence of joint softening in aluminum joints after FSW employing precipitate evolution. Furthermore, Sato et al. [9] studies showed a hardness reduction in the stir zone and thermomechanically affected zone (TMAZ) in aluminum joints undergoing FSW, which they related to the occurrence of recrystallization and grain growth. This effect was later observed by Sarkari Khorrami et al. [10], [11] in HAZ of CGP processed specimens.

The joining of sheet metals in industrial applications notably in automotive industries is generally done via resistance spot welding (RSW). Prashanthkumar et al. [12] derived optimum RSW parameters including weld current and weld time via thermal analysis.

It is worth bearing in mind that welding of aluminum alloys is much more difficult compared to steel alloys because of their high electrical conductivity. Some other common problems of welding of aluminum include porosity in aluminum and its alloys, oxide film on the surface, and hot cracking [13].

Various studies presented evaluations of resistance spot welding through numerical and experimental analysis [14], [15]. It has been shown that generally none of the electrical or thermal methods proposed for monitoring of steel RSW are applicable to aluminum RSW. A method to acquire spot weld parameters including current, voltage, dynamic resistance, electrode displacement, and force was introduced. Although no single-process parameter can be used to predict aluminum weld quality, multiple suitable linear regression methods were presented [16].

In the present work, through different passes of the CGP process, aluminum sheets underwent various strain magnitudes. Following this further, processed sheets were joined through resistance spot welding. Finally, an investigation of the mechanical properties of these sheet metals was conducted through the tensile-shear test. In addition, microhardness values for base metal and fusion zone are derived.

2. Experimental Material and Procedure

In this section, base aluminum sheets used are introduced. Furthermore, the CGP process procedure, preparation of specimens for spot welding, and the spot-welding parameters are described. Finally, the proper setup for the introduction of the CGP process to the sheet metals as well as the tensile-shear test is illustrated.

2.1. Constrained Groove Pressing

The used specimens are 2 mm thick pure 1040 aluminum sheets with yield strength and ultimate tensile strength of 56MPa and 85MPa

respectively. The chemical composition of studied aluminum is presented in Table 1.

Table 1: Studied aluminum component element percentages

Element	Al	Si	Fe	Cu
Percentage	99.44	0.0795	0.37	0.0091
Element	Be	Pb	Sb	Sn
Percentage	0.00004	0.021	0.0017	0.0063
Element	Mn	Mg	Zn	Ti
Percentage	0.0019	0.0091	0.0147	0.022
Element	Zr	Ni	Cr	V
Percentage	0.00085	0.0043	0.0017	0.0148

Initially, severe plastic deformation is achieved through constrained groove pressing, which results in large magnitudes of pre-strains being imposed on the aluminum sheets. The deformation process includes the usage of a corrugated die and a flat die. One CGP pass includes four steps as shown in Figure 1. To begin with, the flat sheet metal undergoes a deformation via the corrugated die resulting in 0.58 effective strain in corrugated regions. In the second step, the corrugated sheet is flattened via the flat die, generating 0.58 strain in the reverse direction on affected regions again. Then, the specimen is turned 180° around its perpendicular axis and subjected to pressing of corrugated and finally flatten die again. This results in non-deformed regions experiencing the same effective strain. A large homogeneous effective strain of 1.16 will be imposed on the sheet after the completion of one pass. By introducing more CGP passes on the specimen, higher plastic strain values can be accumulated without changing the specimen initial dimensions. It should be noted that in the present work aluminum sheet metals with up to four CGP passes are considered.

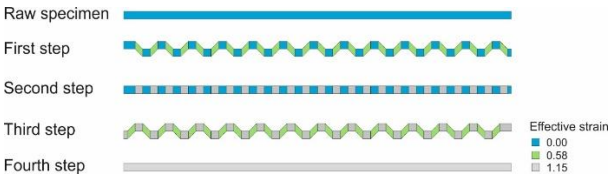

Figure 1: Deformation and effective strain of specimens during the CGP process

2.2. Spot Welding

Resistance spot welding is a fusion process that requires the application of both heat and pressure to achieve an appropriate joint. The pressure is provided by means of clamping two or more overlapping sheets between two electrodes, then a current flows between electrodes. Melting occurs after the generation of sufficient heat at the interface. This heat is produced because of the resistance of workpieces, contact resistance of workpieces against the current, and resistance between electrodes and workpieces. A weld nugget is then formed and an autogenous fusion weld is made between the plates [13].

CGPed Aluminum sheets are machined at both sides to a thickness of 1.4mm to achieve a smooth surface appropriate for spot welding. Following this further, the specimens are prepared according to the AWS C1.1M/C1.1:2012 standard [17]. A single-phase DC welding machine is used to perform the welding process, which is carried out using electrodes with a face diameter of 6mm. Throughout all tests, the welding time and welding force are evenly maintained. The welding current is increased in 1kA steps starting from 26kA to 30kA.

Evaluation of quality of spot welds mainly depends on three parameters including fusion zone size, weld mechanical performance, and failure mode. Fusion zone size, itself, depends on weld penetration and nugget diameter. The static mechanical performance of spot weld is measured by means of the value of peak load obtained via the tensile-shear test [2].

Tensile-shear test specimens, dimensions of which are illustrated in Figure 2, are prepared according to the AWS C1.1M/C1.1:2012 standard [17].

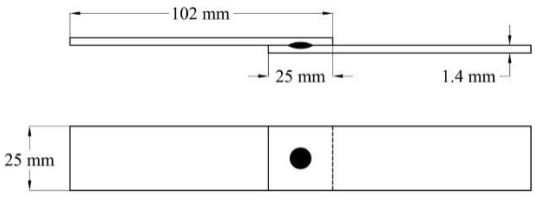

Figure 2: Dimensions of specimens for the welding process

Tensile-shear tests are performed with a constant speed of 5 mm/min via a Santam machine. Figure 3 illustrates the schematics of the tensile-shear test specimen setup during the test. As can be seen in Figure 3, a 1.4mm spacer is

placed between the sample sheet and the jaw to prevent bending during the test.

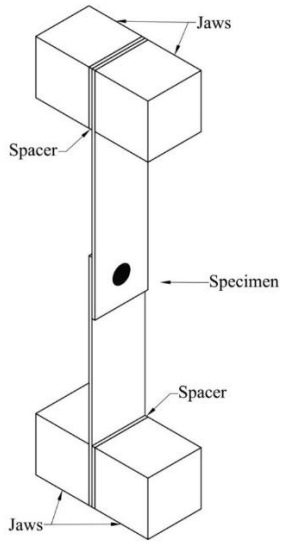

Figure 3: Schematics of tensile-shear test

An important criterion to evaluate the quality of spot weld is the failure mode. In this case, two different modes of failure include interfacial failure (IF) and pullout failure (PF), which are presented in Figure 4. The former failure stems from a crack through the fusion zone resulting in separation, in the latter a piece or in severe cases the whole nugget separates from one sheet. In comparison to the IF failure mode, the occurrence of PF failure mode drastically increases the load-carrying capacity of the RSWed joints, thus it is considered the ideal failure mode. The failure modes are evaluated after complete separation during tensile-shear tests.

Figure 4: Failure modes. Left: IF failure mode - Right: PF failure mode

The microhardness variation is measured on the thickness cross-sections through the centerline of the weld as depicted in Figure 5.

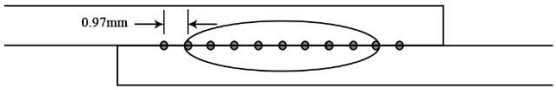

Figure 5: Vickers microhardness measurement profile through the cross-section of welded specimens

3. Results and Discussion

3.1 Tensile-Shear Test

The tensile-shear test results are illustrated in Figure 6. Annealed aluminum specimens are referred to as anneal, specimens with one pass of CGP as CGP1, specimens with two passes of CGP as CGP2, specimens with three passes of CGP as CGP3 last but not least specimens with four passes of CGP as CGP4.

Results lead to the conclusion that the strength of specimens increases as the number of CGP passes increases. In comparison to the annealed specimen, at the first CGP pass, the yield strength shows a 78% increase, at CGP2 experiences the maximum increase at near 90% while the ultimate strength increases 18% and 24% at CGP1 and CGP2 respectively.

3.2 Tensile-Shear Test of Welded Specimens

A tensile-shear test for single lap welded joints for annealed and CGP1 through CGP4 specimens was carried out. The welding current was increased in 1kA steps starting from 26kA until pullout failure mode was observed at 30kA for a CGP4 specimen. Tensile-shear test results are shown in Figures 7 to 11 at currents constant at 26, 27, 28, 29, and 30kA respectively. The welding time and welding force are considered constant parameters during the spot weld process of specimens.

It can be seen that both welding current and CGP pass number have a major effect on welding strength. As can be seen in Figure 7, before slowing down noticeably, peak load increases for the first two CGP passes, 25% and 120% for CGP1 and CGP2 respectively in comparison to the annealed specimen. A significant improvement in the maximum load-carrying capacity of the joints is observed when the welding current is changed from 27kA to 28kA. This improvement trend continues as the weld current increases.

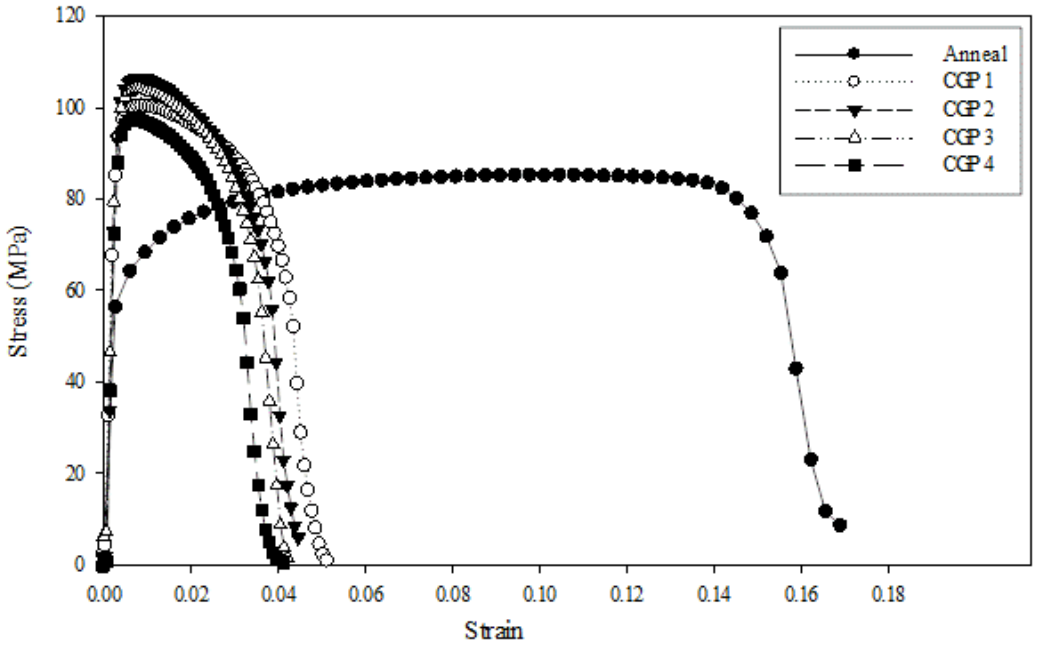

Figure 6: Tensile test results of anneal and CGPed specimens

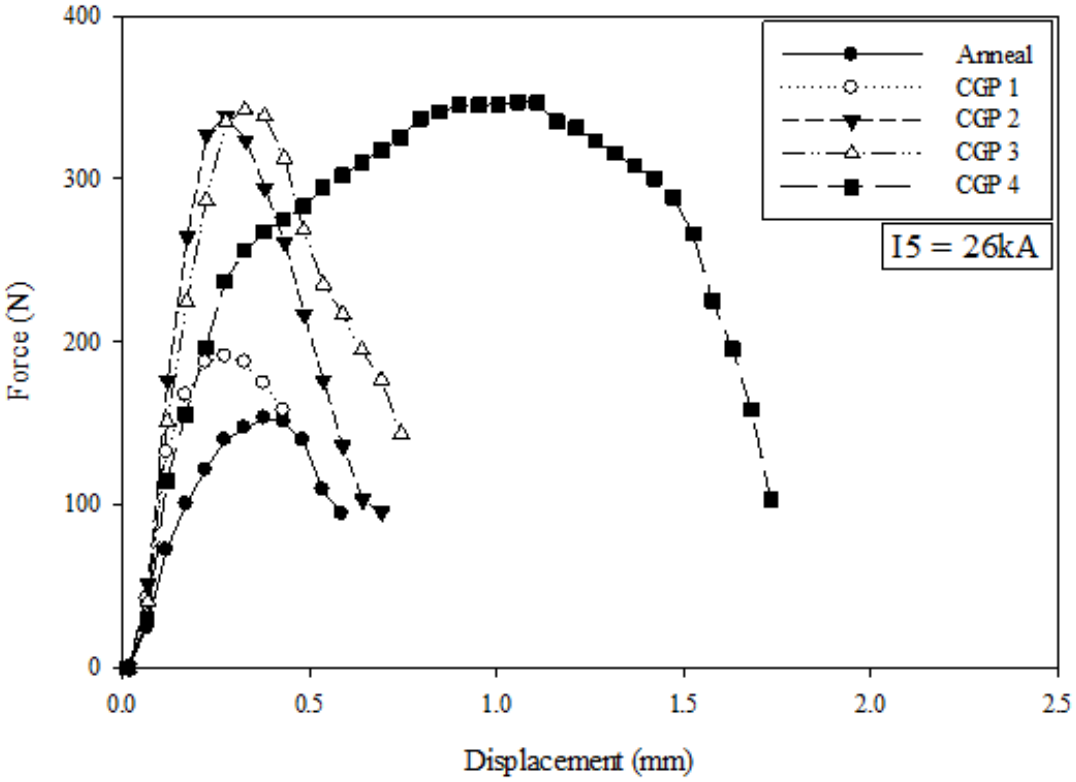

Figure 7: Tensile-shear test result of welded single lap joints for welding current of 26kA

It is also of importance that CGP4 welded joints experienced almost 3 times higher displacement before failure at 26kA. Overall, a growth trend can also be observed for displacement before failure as the welding current increases.

Maximum displacement before failure rises from 1.73mm to 4.95mm for 26kA and 30kA respectively. It's worth bearing in mind that this maximum always occurred for CGP4.

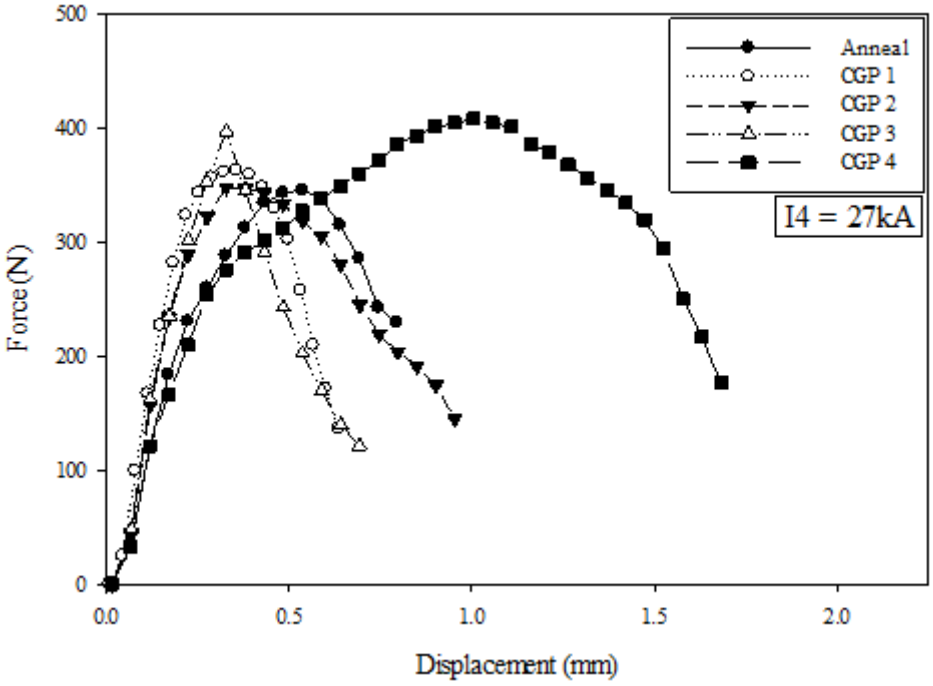

Figure 8: Tensile-shear test result of welded single lap joints for welding current of 27kA

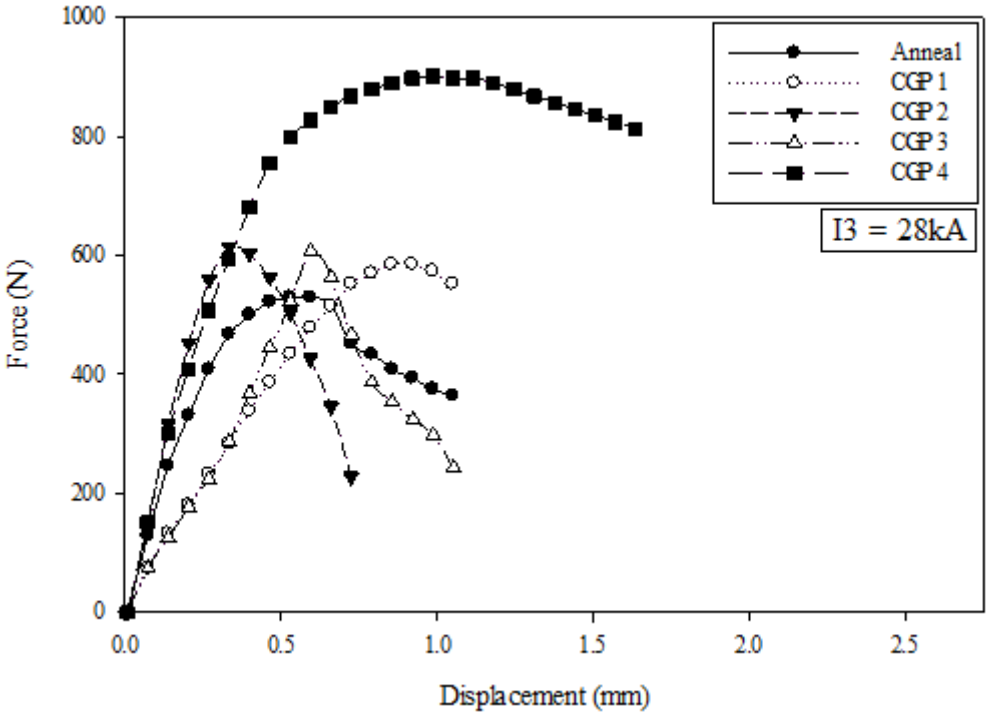

Figure 9: Tensile-shear test result of welded single lap joints for welding current of 28kA

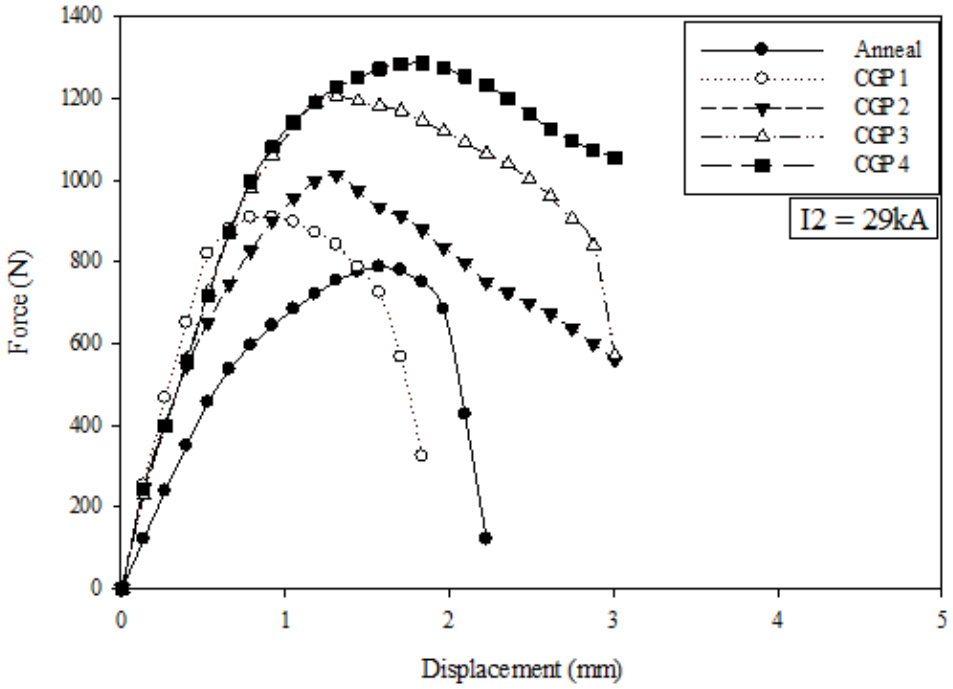

Figure 10: Tensile-shear test result of welded single lap joints for welding current of 29kA

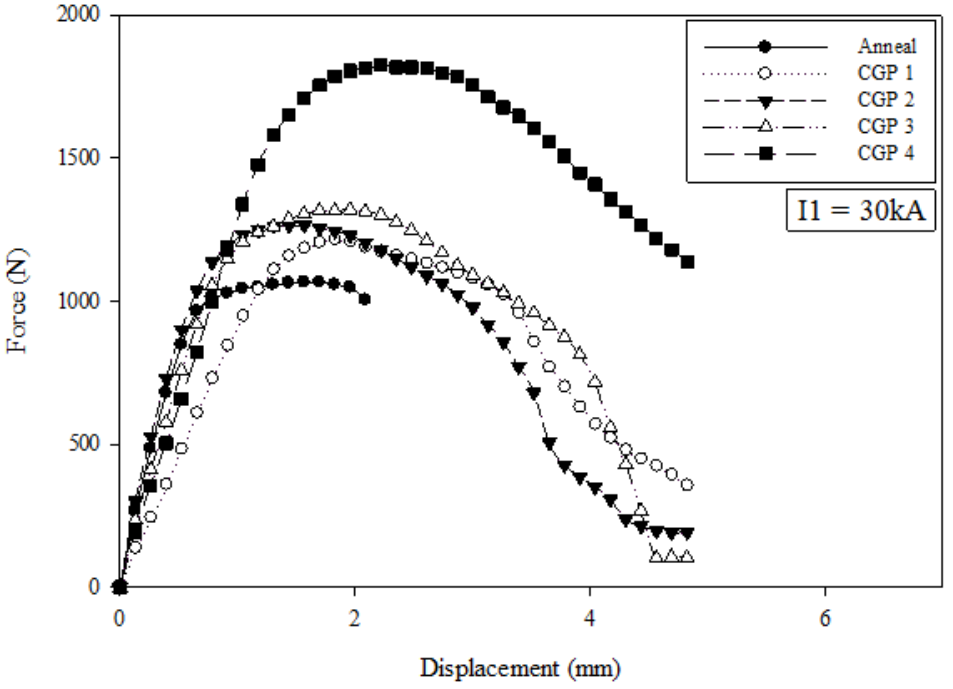

Figure 11: Tensile-shear test result of welded single lap joints for welding current of 30kA

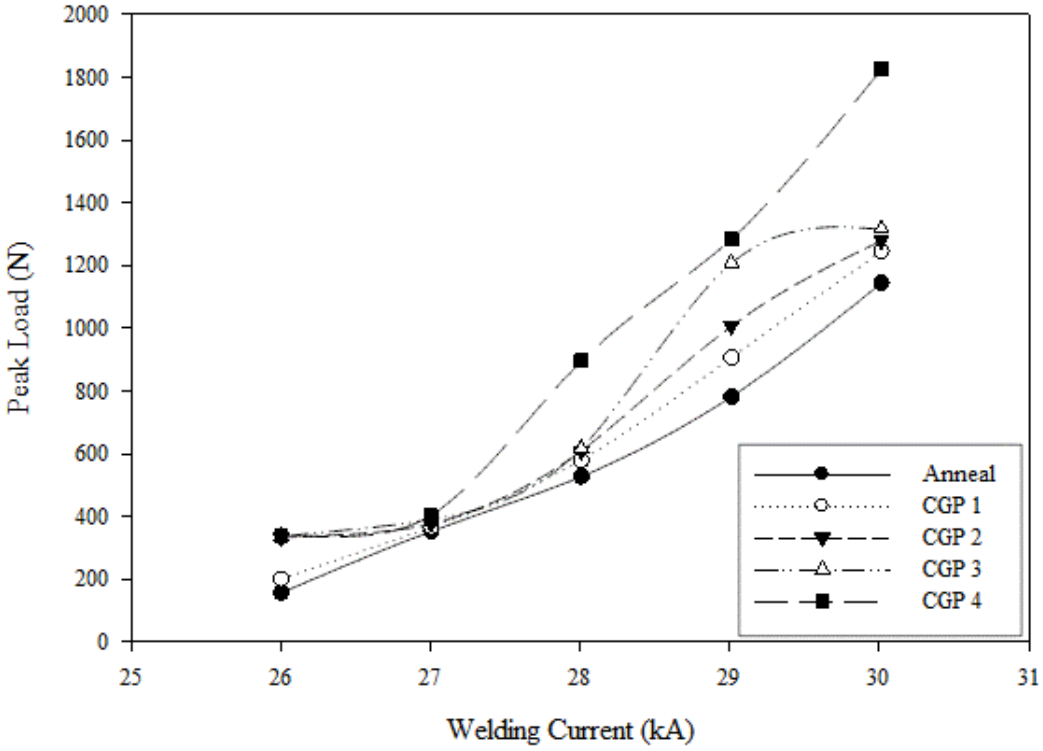

Figure 12: Peak load vs welding current for various CGP passes of welded single lap joints

Figure 11 illustrates the effect of the failure mode on joints load-carrying capacity. After CGP4 welded joints experienced pullout failure mode, the load-carrying capacity of the joint shows an increase of 38% from CGP3 specimen welded at the same current. Comparing these results to a CGP4 joint welded at 26kA and an annealed joint welded at 26kA, load carrying capacity is 5 times and 12 times greater in magnitude.

The effects of welding current on peak load during tensile shear tests are illustrated in Figure 12. It can be concluded that increasing the welding current for each CGP pass increases peak load. At CGP4 increasing current by 4kA from 26kA to 30kA leads to a peak load more than 5 times greater. It is also of importance that increasing CGP passes results in higher peak load magnitude at a constant welding current. Furthermore, it can be seen that peak load is higher in CGP4 throughout the different weld currents.

Bearing in mind that peak load is in direct relation to the mechanical performance of a welded joint, this provides a strong ground for the CGP process improving the RSW of aluminum specimens.

3.3 Failure Behavior

The failure mode has a great effect on the load-carrying capacity of spot welds. Two different failure behavior was observed after the static tensile-shear test. A model of stress distribution at the weld zone is depicted in Figure 13.

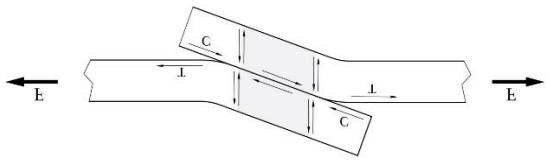

Figure 13: Stress distribution at the weld zone for a welding specimen

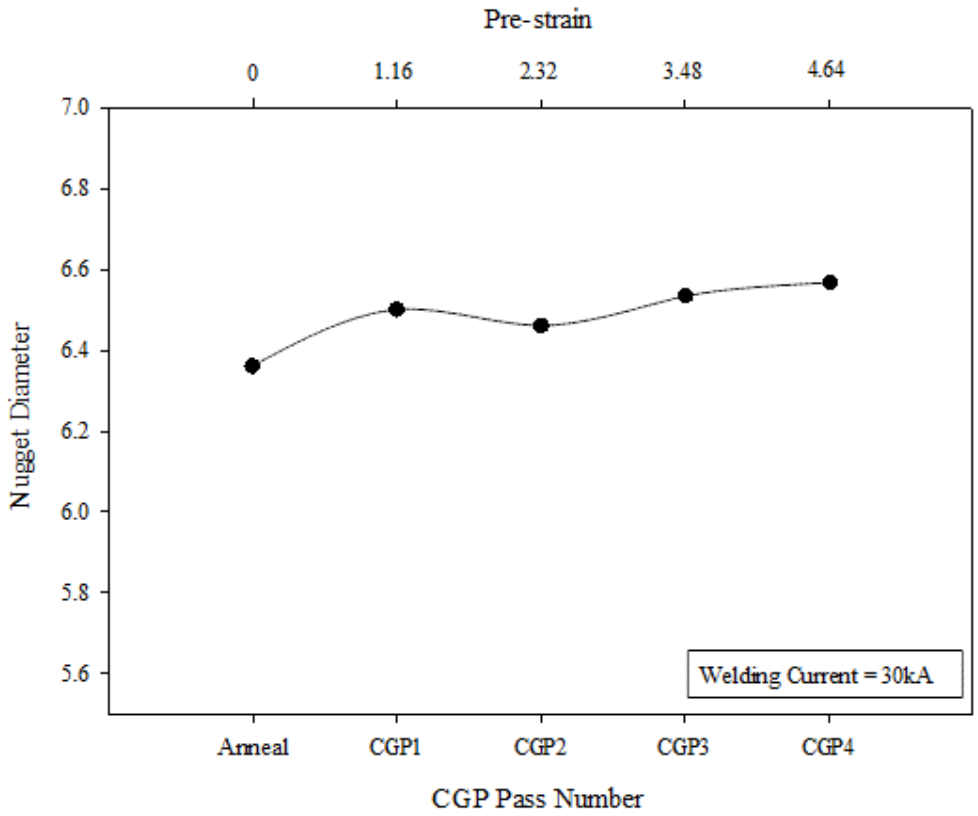

Figure 14: Nugget diameter versus CGP pass number of specimens welded at 30kA welding current

During the separation, the dominant factor in the case of interfacial failure mode is shear stress, however, tensile stress is the dominant factor in the case of pullout failure mode. Overlapping of sheets and rotation of the weld nugget in response to the inflicted force, generates a bending moment, which results in tensile stress during the tensile-shear test. It is worth bearing in mind that **T** in Figure 13 represents tensile normal stresses while **C** is compressive normal stresses. Experiments were carried out until the pullout failure mode was observed. Pullout failure occurred for CGP4 welded specimen in welding current of 30kA.

3.4 Nugget Diameter

An upward trend of nugget diameter can be observed in Figure 14 as the CGP passes increase. Nugget diameter growth slows down noticeably after an initial surge at CGP1. Nugget diameter is in direct relation with the size of the fusion zone. A greater fusion zone results in higher strength joints that can endure higher peak loads.

Nugget diameter is in direct relation with heat input, which can be obtained via [18]:

$$Q = RI^2t \quad (1)$$

Where Q is heat input, R is sheet resistance, I and t weld current, and weld time respectively. In a constant current and weld time, sheet resistance increase results in heat input increase. Total resistance between electrodes include resistance between electrodes and workpieces, the resistance of workpieces, and contact resistance of workpieces against the current, the two latter are key factors for the most part, and interface contact resistance is mainly dependent on

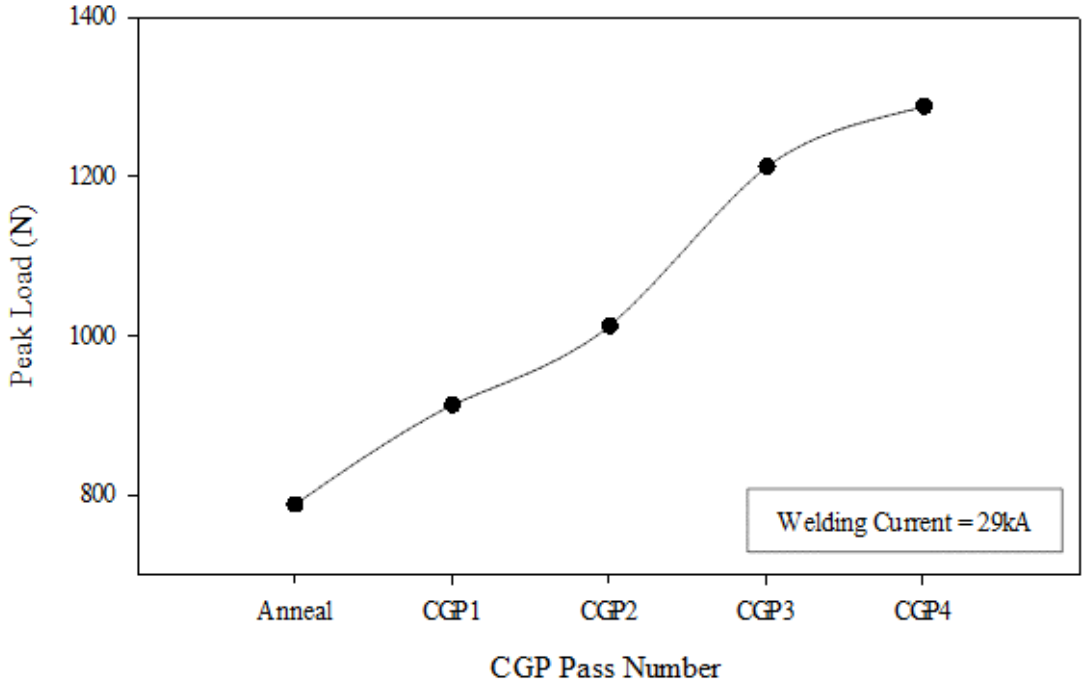

Figure 15: Peak load versus CGP pass number of specimens welded at 29kA welding current

surface finish. According to [18] sheet resistance can be computed as:

$$R = \rho \frac{l}{s} \tag{2}$$

Where R is sheet resistance, ρ electrical resistivity, l and s are length, in this case, the thickness of sheets, and electrode diameter respectively. Given constant l and s, the sheet resistance is increased through the increase of electrical resistivity, so Figure 14 and (1) and (2) leads to the conclusion that increasing CGP passes in fact increase electrical resistivity of aluminum sheets.

3.5 Peak Load

According to the tensile-shear test results the peak load correlates to the point of crack propagation through the nugget in IF mode and the necking point for PF mode during the failure [19]. The variation of peak load versus CGP pass number in a constant welding current is depicted in Figure 15. Results support the idea that the increase of the CGP pass number is in direct relation to the peak load increase given constant welding parameters.

3.6 Micro Hardness Measurements

The variation of the hardness of spot welds throughout the region of effect alongside the base metal is represented in Figure 16 for annealed and different CGP passes. Through base metal and region of effect, the variation of microhardness in annealed specimens is very minute. However, after experiencing a sharp drop in HAZ in comparison to the base metal, CGPed specimens' microhardness values near the value of annealed specimen in the fusion zone. In the fusion zone, CGPed specimens behave as if they were annealed. Furthermore, Figure 16 shows that CGPed specimens possess better microhardness in base metal as well as in fusion zone due to work hardening and refinement of grains [20].

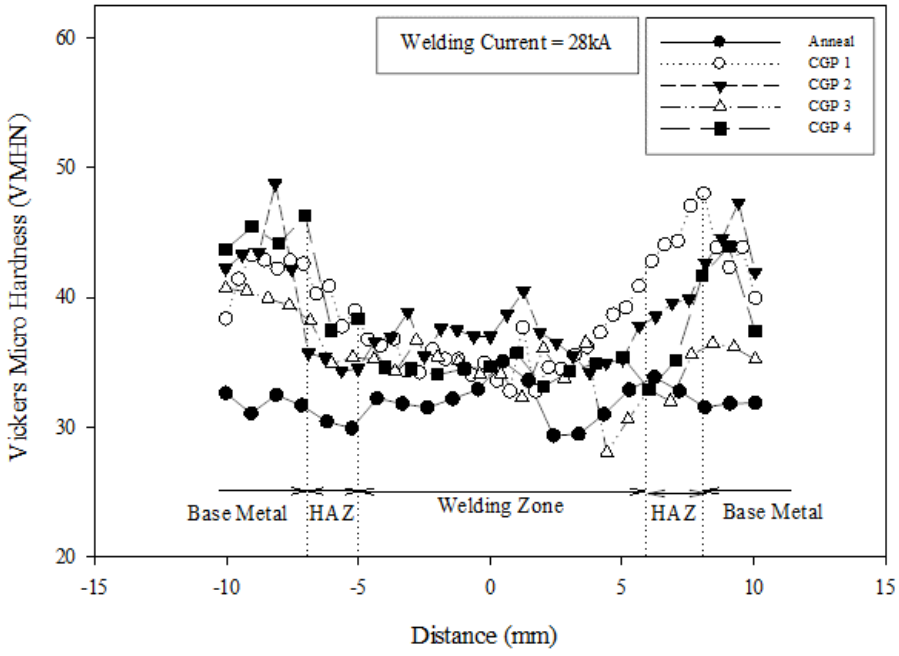

Figure 16: Microhardness values along various locations of the joint

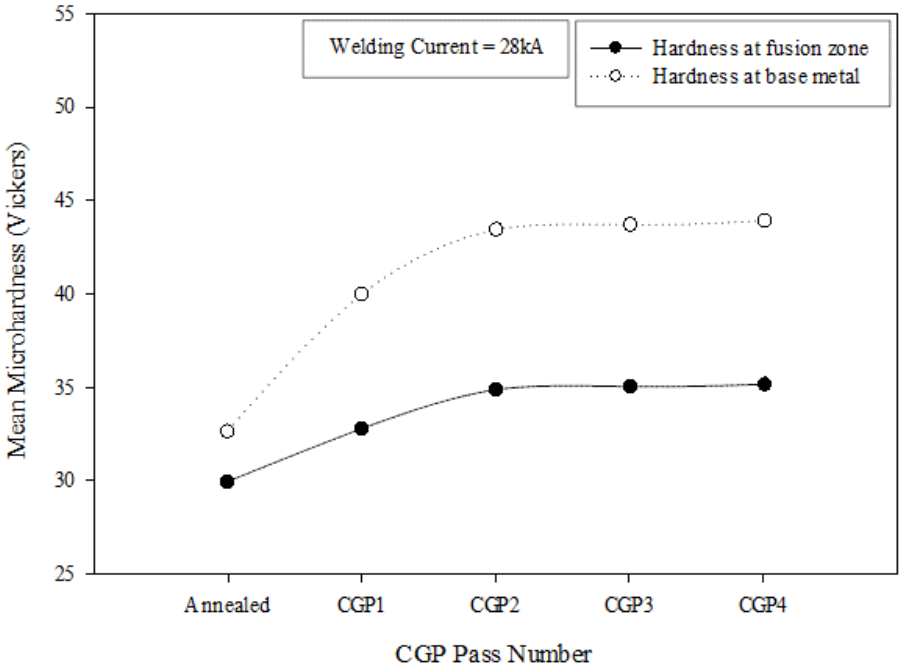

Figure 17: Mean microhardness values for various CPG pass numbers.

4. Conclusions

The main objective of this study is the research and evaluation of resistance spot weld on CGPed aluminum specimens. The mechanical responses and the behavior of failure of the joints are investigated, the results can be summarized as follows:

1. The CGP process can efficiently increase the strength of spot-welded joints of aluminum sheet metals
2. CGP process on aluminum sheets improves welding mechanical characteristics including nugget diameter, peak load, and weld parameters.
3. The welding current and CGP pass number are dominant factors increasing the strength of the joint and the quality of mechanical behavior of the weld during the tensile-shear test.
4. For a constant welding current, CGPed specimens exhibit higher microhardness, which experiences a drop in HAZ. Furthermore, increasing of CGP pass number results in higher microhardness values overall.

References

[1] M. Zehetbauer and R. Z. (Ruslan Z. Valiev, Nanomaterials by severe plastic deformation : proceedings of the conference "Nanomaterials by Severe Plastic Deformation, NANOSPD2," December 9-13, 2002, Vienna Austria. Wiley-VCH, 2004.

[2] F. Khodabakhshi, M. Kazeminezhad, and A. H. Kokabi, "Mechanical properties and microstructure of resistance spot welded severely deformed low carbon steel," Mater. Sci. Eng. A, vol. 529, pp. 237–245, Nov. 2011.

[3] D. H. Shin, J.-J. Park, Y.-S. Kim, and K.-T. Park, "Constrained groove pressing and its application to grain refinement of aluminum," Mater. Sci. Eng. A, vol. 328, no. 1–2, pp. 98–103, May 2002.

[4] H. S. Googarchin, B. Teimouri, and R. Hashemi, "Analysis of constrained groove pressing and constrained groove pressing-cross route process on AA5052 sheet for automotive body structure applications," Proc. Inst. Mech. Eng. Part D J. Automob. Eng., vol. 233, no. 6, pp. 1436–1452, May 2019.

[5] M. Kazeminezhad and E. Hosseini, "Optimum groove pressing die design to achieve desirable severely plastic deformed sheets," Mater. Des., vol. 31, no. 1, pp. 94–103, Jan. 2010.

[6] A. Shirdel, A. Khajeh, and M. M. Moshksar, "Experimental and finite element investigation of semi-constrained groove pressing process," Mater. Des., vol. 31, no. 2, pp. 946–950, Feb. 2010.

[7] A. Sajadi, M. Ebrahimi, and F. Djavanroodi, "Experimental and numerical investigation of Al properties fabricated by CGP process," Mater. Sci. Eng. A, vol. 552, pp. 97–103, Aug. 2012.

[8] Y. C. Chen, J. C. Feng, and H. J. Liu, "Precipitate evolution in friction stir welding of 2219-T6 aluminum alloys," Mater. Charact., vol. 60, no. 6, pp. 476–481, Jun. 2009.

[9] Y. S. Sato, Y. Kurihara, S. H. C. Park, H. Kokawa, and N. Tsuji, "Friction stir welding of ultrafine grained Al alloy 1100 produced by accumulative roll-bonding," Scr. Mater., vol. 50, no. 1, pp. 57–60, Jan. 2004.

[10] M. Sarkari Khorrami, M. Kazeminezhad, and A. H. Kokabi, "Microstructure evolutions after friction stir welding of severely deformed aluminum sheets," Mater. Des., vol. 40, pp. 364–372, Sep. 2012.

[11] M. Sarkari Khorrami, M. Kazeminezhad, and A. H. Kokabi, "The effect of SiC nanoparticles on the friction stir processing of severely deformed aluminum," Mater. Sci. Eng. A, vol. 602, pp. 110–118, Apr. 2014.

[12] V. K. Prashanthkumar, N. Venkataram, N. S. Mahesh, and Kumarswami, "Process Parameter Selection

for Resistance Spot Welding through Thermal Analysis of 2 mm CRCA Sheets," Procedia Mater. Sci., vol. 5, pp. 369–378, Jan. 2014.

[13] G. Mathers, The welding of aluminium and its alloys. CRC Press, 2002.

[14] S. Zhang, "A Simplified Spot Weld Model for Finite Element Analysis," 2004.

[15] S. Zhang, "Simplified Spot Weld Model for NVH Simulations," 2005.

[16] M. Hao, K. A. Osman, and D. R. Boomer, "Development in characterization of resistance spot welding of aluminum." American Welding Society, Miami, FL (United States), 31-Dec-1994.

[17] A. W. S. C. on A. Welding, "Recommended Practices for Resistance Welding," 1966.

[18] H. Zhang, J. Senkara, and J. Senkara, Resistance Welding. CRC Press, 2011.

[19] M. Pouranvari, A. Abedi, P. Marashi, and M. Goodarzi, "Effect of expulsion on peak load and energy absorption of low carbon steel resistance spot welds," Sci. Technol. Weld. Join., vol. 13, no. 1, pp. 39–43, Jan. 2008.

[20] F. Khodabakhshi, M. Kazeminezhad, and A. H. Kokabi, "Constrained groove pressing of low carbon steel: Nano-structure and mechanical properties," Mater. Sci. Eng. A, vol. 527, no. 16–17, pp. 4043–4049, Jun. 2010.